(**8**). We are carrying out ab initio SCF–MO calculations to compare total energies of **6** and **10**.

In the double DSD process, eq 2, the degree of coordination at the vertices is preserved because the two switching edges are perpendicular to each other and involve a common vertex, in this case vertex 1. Switching edge 1,7 to 4,6 creates new caps at 1 and 7 and converts old caps at 4 and 6 into prism vertices. Simultaneously, the switch of the perpendicular edge from 2,3 to 1,5 forms new caps at 2 and 3 and turns the former cap at 5 and the incipient cap at 1 into prism vertices, preserving three caps and six prism vertices. For a double DSD process, one vertex must be common to both bond breaking and bond forming at the two switching edges. As a counterexample consider the process in which bonds 2,8 and 3,9 break in **1** to form two squares faces sharing the common vertex 5. The resulting structure (**11**) has

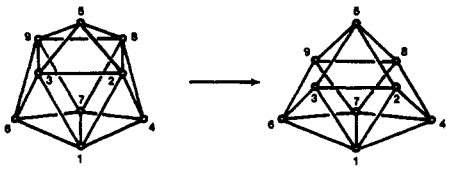

1 **11**

C_{2v} symmetry and is identical, except for labeling, with **6**. But as Guggenberger and Muetterties pointed out,[14] formation of new bonds in **11** will not carry this structure into a tricapped trigonal prism, and therefore this process will not lead to a DSD isomerization. Equations 1 and 2 appear to be the only DSD processes that regenerate the starting polyhedron with an exchange of vertex labels.[28]

Conclusions

We have shown that for $B_9H_9^{2-}$ and $C_2B_7H_9$ the single DSD process, eq 1, is forbidden by orbital symmetry while the double DSD mechanism, eq 2, is allowed. On the basis of qualitative considerations, we can conclude that energy barriers must separate the three lowest energy $C_2B_7H_9$ isomers on the loop or cycle connecting rearrangements that follow eq 2. The results of ab initio SCF–MO calculations suggest that these barriers might be large enough to allow isolation of the lowest energy isomers, if indeed rearrangement takes place by eq 2. Only a single isomer is known experimentally.

Theoretical analyses of DSD framework reorganizations have previously been reported for B_4H_4 (symmetry-forbidden but unknown experimentally),[29,30] for $B_5H_5^{2-}$ (symmetry-forbidden; experimentally known to be rigid),[24] and for $B_8H_8^{2-}$ and $B_{11}H_{11}^{2-}$ (symmetry-allowed; experimentally fluxional).[31,32] PRDDO–MO calculations have been reported for possible mechanisms for the observed interconversion of the two $C_2B_4H_6$ isomers.[33] There is experimental evidence for DSD rearrangements in $C_2B_5H_7$.[34] Lipscomb has suggested that polyhedral rearrangements occurring at high temperature might involve symmetry crossings of molecular orbitals.[35]

The DSD framework rearrangement proposal has stimulated productive research for 20 years. We now know that such rearrangements very likely occur in some systems but not in others. As in all mechanistic processes, Nature does not always allow reactants to follow the paths that chemists find most appealing and most readily visualized.

Registry No. $B_9H_9^{2-}$, 12430-24-9; $C_2B_7H_9$, 26998-72-1.

(28) One of the reviewers pointed out that, to be absolutely certain on this point, one would have to examine each of the 2606 combinatorially distinct 9-atom polyhedra. See: Duijvestijn, A. J. W.; Federico, P. J. *Math. Comput.* **1981**, *37*, 523.

(29) Kleier, D. A.; Bicerano, J.; Lipscomb, W. N. *Inorg. Chem.* **1980**, *19*, 216–218.
(30) McKee, M. L.; Lipscomb, W. N. *Inorg. Chem.* **1981**, *20*, 4148–4151.
(31) Kleier, D. A.; Lipscomb, W. N. *Inorg. Chem.* **1979**, *18*, 1312–1318.
(32) Kleier, D. A.; Dixon, D. A.; Lipscomb, W. N. *Inorg. Chem.* **1978**, *17*, 166–167.
(33) Halgren, T. A.; Pepperberg, I. M.; Lipscomb, W. N. *J. Am. Chem. Soc.* **1975**, *97*, 1248–1250.
(34) Abdou, Z. J.; Soltis, M.; Oh, B.; Siwap, G.; Banuelos, T.; Nam, W.; Onak, T. *Inorg. Chem.* **1985**, *24*, 2363–2367.
(35) Lipscomb, W. N. *Boron Chemistry 4*; Parry, R. W., Kodama, G., Eds.; Pergamon: London, 1980; p 1.

Contribution from the Lehrstuhl für Theoretische Chemie, Technische Universität München, D-8046 Garching, Federal Republic of Germany

On the Electronic Structure of Metal Tetrahydroborates: Quasi-Relativistic Xα–SW Study of $M(BH_4)_4$ (M = Zr, Hf, Th, U)

D. Hohl and N. Rösch*

Received December 9, 1985

Quasi-relativistic SCF–Xα scattered-wave calculations are presented for the series of metal tetrakis(tetrahydroborates) $M(BH_4)_4$ (M = Zr, Hf, Th, U). The bonding in the transition-metal compounds is that of tetrahedral d^0 complexes with strong covalent contributions from π bonding ligand group orbitals. In the actinide complexes, 5f orbitals of the central atom are found to be important to covalent ligand–metal bonding but less than in the corresponding di-π-[8]annulene compounds. The ligand field manifold of $U(BH_4)_4$ and the corresponding spin–orbit constant agree well with experimental data. Photoelectron spectra are reproduced satisfactorily with the exception of a uniform shift. An explanation is presented why the first ligand-derived band in the spectra of the actinide complexes is narrower than that in the transition-metal compounds. The difference between the zirconium and hafnium complexes in the splitting of the second band is found to be a relativistic effect due to a more effective covalent mixing of the Hf 6s orbital.

Introduction

Recent molecular orbital studies[1,2] have shown that f orbitals of actinides and lanthanides contribute to covalent bonding in complexes containing the [8]annulene ligand. Fairly sizable f covalency effects have been identified for uranocene ((di-π-[8]-annulene)uranium(IV)),[1,2] and somewhat smaller effects for thorocene and cerocene.[2,3] It is of considerable interest whether such bonding is unique to this type of molecule or whether it may

(1) Rösch, N.; Streitwieser, A., Jr.; *J. Am. Chem. Soc.* **1983**, *105*, 7237.
(2) Rösch, N. *Inorg. Chim. Acta* **1984**, *94*, 297.
(3) Streitwieser, A., Jr.; Kinsley, S. A.; Rigsbee, J. T.; Fragala, I.; Ciliberto, E.; Rösch, N. *J. Am. Chem. Soc.* **1985**, *107*, 7786.

0020-1669/86/1325-2711$01.50/0

Table I. Bond Lengths,[a] Bond Angles,[a] and Muffin-Tin Sphere Radii[a] Used in the Calculations for Various Complexes $M(BH_4)_4$

M	Zr	Hf	Th	U
d(M-B)	2.308	2.281	2.570	2.520
$d(B-H_t) = d(B-H_b)$[b]	1.250	1.250	1.250	1.250
$\angle H_bBH_b$	107	107	107	107
$\angle H_bBH_t$	113	113	113	113
r(M)	1.484	1.457	1.746	1.696
r(B)	0.824	0.824	0.824	0.824
$r(H_b) = r(H_t)$	0.427	0.427	0.427	0.427

[a] All lengths in angstroms; all angles in degrees. [b] Terminal hydrogen atoms denoted by H_t; bridging ones, by H_b.

also be found in other actinide and lanthanide compounds.

A quite different class of compounds forming possible candidates for a comparable involvement of f orbitals are the metal tetrakis(tetrahydroborates), $M(BH_4)_4$.[4] They exhibit physical and chemical properties that are typical for covalent molecules, like high volatility and solubility in nonpolar solvents. Of the seven known metal tetrakis(tetrahydroborates) five are actinide compounds (Th through Pu), the others containing transition metals (Zr and Hf). In the vapor phase all of them are monomeric and may be assumed to exhibit ideal tetrahedral symmetry (T_d) with each of the four borohydride ligands being linked to the central metal atom via three bridging hydrogen atoms.[5,6] This structure is ideally suited for a molecular orbital analysis of the bonding. In the solid state Th, Pa, and U tetrahydroborates are polymeric and 14-coordinate with two tridentate and four bridging bidentate BH_4^- groups around the central metal,[6,8] whereas the Zr, Hf, Np, and Pu tetrahydroborates are monomeric 12-coordinate complexes.[4,6,9,10] Crystalline monomeric 12-coordinate tetrakis(methyltrihydroborato) compounds of Zr, Th, U, and Np have also been synthesized.[11] Of all these compounds a wide variety of physical, chemical, optical, and magnetic data have been recorded.[6,11-14] It is therefore somewhat surprising that no systematic theoretical study of the electronic structure of the metal tetrakis(tetrahydroborates) has been undertaken so far.

In the following we will present results of quasi-relativistic molecular orbital calculations for the molecules $M(BH_4)_4$ (M = Zr, Hf, Th, U). Both actinide and transition-metal tetrahydroborates were included in our investigations to obtain a more thorough understanding of the possible role of f orbitals as well as of relativistic effects. Previous theoretical discussions[12,15,16] of such compounds were mainly based on qualitative molecular orbital arguments, e.g. on the isolability principle[17] comparing the ligands η^3-BH_4^-, Cl^-, and η^5-$C_5H_5^-$.[16] To our knowledge, only one calculation has been performed previously, namely for Zr-$(BH_4)_4$ using the LCAO-DVM-Xα method.[15]

Computational Details

The calculations have been performed by using the SCF-Xα scattered-wave (SW) method[18,19] in a quasi-relativistic form,[20,21] which has proven well suited for large molecules containing heavy elements.[1-3,20] Since the quasi-relativistic approximation properly reduces to the familiar nonrelativistic Xα-SW method for light elements,[2,20] all complexes were studied within the same theoretical framework. All molecules $M(BH_4)_4$ (M = Zr, Hf, Th, U) were considered tetrahedral with ideal T_d point group symmetry. Metal-boron distances were taken from known structures for M = Zr,[9] Hf,[10] and U.[8] For M = Th the bond distance was deduced via a comparison of atomic radii for Th and U.[22] The resulting distance is also compatible with X-ray structural data for the corresponding methylborohydride compound.[11] For the borohydride ligand an idealized average geometry was derived from $U(BH_4)_4$ data and employed uniformly for the various complexes. Pertinent bond distances and angles are collected in Table I.

Since the metals under consideration exhibit a considerable range of atomic radii,[22] no uniform muffin-tin geometry could be chosen for all calculations—a device that has proven so useful in previous investigations.[1,2] For the BH_4^- ligand one set of muffin-tin radii was used in all calculations to facilitate the desired comparison of different metal complexes. In this way the muffin-tin errors inherent to the scattered-wave method are hopefully kept as uniform as possible. For the uranium complex the metal-boron distance was partitioned according to the ratio of the corresponding atomic radii.[22] All other radii were then determined by requiring touching spheres. The resulting muffin-tin radii are displayed in Table I.

The molecules under consideration exhibit a fairly open structure, and the muffin-tin approximation to the electronic potential will undoubtedly limit the accuracy of the present investigations. A popular method to partially correct for such errors is the use of overlapping spheres.[23,24] As an indicator for these errors one may take the large delocalization of the ligand-derived orbitals into the interatomic region observed in the present study (see Table II) and a fairly uniform shift of the calculated ionization potentials (see Table VI). To estimate the size of the muffin-tin errors and their effect on the level structure, various sets of sphere radii have been investigated for uranium borohydride.[25] The main effect observed was an almost parallel shift of the orbital energy spectrum. Fairly good agreement with experimental ionization potentials (deviating less than 0.5 eV) could be obtained by following Norman's procedure for choosing overlapping sphere radii based on a reduction factor of 0.85.[24] However, it was felt that the corresponding sphere radii (r(U) = 1.545 Å, r(B) = 0.974 Å, r(H) = 0.751 Å) induce a very uneven distribution of the molecule featuring a rather small metal sphere and an extreme overlap of 38% between boron and hydrogen spheres. Since it is not the intention of the present theoretical study to fit experimental data, we have chosen the parametrization as rationalized above.

The maximum l values in the scattered-wave expansions included were l = 3 in the metal sphere, l = 1 for B, l = 0 for H, and l = 5 in the extramolecular region.

The atomic exchange parameters α were taken from the values tabulated by Schwarz[26] or extrapolated from then (α(Th) = α(U) = 0.692). The exchange scaling parameters for the intersphere and the extramolecular region were taken as weighted averages over the corresponding atomic parameters.[18] The core electron densities for B ([He]), Zr ([Ar]$3d^{10}$), Hf ([Kr]$4d^{10}$), and Th and U ([Xe]$4f^{14}5d^{10}$) were kept frozen at their atomic values as obtained from relativistic Xα calculations. All other electrons were considered fully in the quasi-relativistic SCF calculations, spin-orbit coupling being neglected. For reasons of uniformity and simplicity we will report below the results of the calculations on $U(BH_4)_4$ obtained without spin polarization. These results essentially agree with those of a spin-polarized calculation except for the obvious population change within the U 5f manifold (see below). Ionization potentials were calculated by using Slater's "transition state" procedure.[18]

To evaluate the ligand-metal interaction and to isolate the corresponding level shifts from muffin-tin induced effects, a $(BH_4)_4$ cluster with an empty sphere in place of the metal has also been calculated from the same geometry as for the uranium complex. For further comparison, results of an Xα-SW calculation of UCl_4 will also be mentioned. The corresponding computational details and a further discussion focusing on

(4) Marks, T. J.; Kolb, J. R. *Chem. Rev.* **1977**, *77*, 263.
(5) James, B. D.; Smith, B. E.; Wallbridge, M. G. H. *J. Mol. Struct.* **1972**, *14*, 327.
(6) Banks, R. H.; Edelstein, N. M. *ACS Symp. Ser.* **1980**, *No. 131*, 331.
(7) Hoekstra, H. R.; Katz, J. J. *J. Am. Chem. Soc.* **1949**, *71*, 2488.
(8) Bernstein, E. R.; Hamilton, W. C.; Keiderling, T. A.; LaPlaca, S. J.; Lippard, S. J.; Mayerle, J. J. *Inorg. Chem.* **1972**, *11*, 3009.
(9) Plato, V.; Hedberg, K. *Inorg. Chem.* **1971**, *10*, 590.
(10) Broach, R. W.; Chuang, I.; Marks, T. J.; Williams, J. *Inorg. Chem.* **1983**, *22*, 1081.
(11) Shinomoto, R.; Gamp, E.; Edelstein, N. M.; Templeton, D. H.; Zalkin, A. *Inorg. Chem.* **1983**, *22*, 2351.
(12) Downs, A. J.; Egdell, R. G.; Orchard, A. F.; Thomas, P. D. P. *J. Chem. Soc., Dalton Trans.* **1978**, 1755.
(13) Rajnak, K.; Gamp, E.; Shinomoto, R.; Edelstein, N. M. *J. Chem. Phys.* **1984**, *80*, 5942.
(14) Rajnak, K.; Gamp, E.; Shinomoto, R.; Edelstein, N. M. *Inorg. Chim. Acta* **1984**, *95*, 29. Gamp, E.; Edelstein, N. M. *J. Chem. Phys.* **1984**, *80*, 5963.
(15) Hitchcock, A. P.; Hao, N.; Werstiuk, N. H.; McGlinchey, M. J.; Ziegler, T. *Inorg. Chem.* **1982**, *21*, 793.
(16) Mancini, M.; Bougeard, P.; Burns, R. C.; Mlekuz, M.; Sayer, B. G.; Thompson, J. I. A.; McGlinchey, M. J. *Inorg. Chem.* **1984**, *23*, 1072.
(17) Hoffmann, R. *Angew. Chem., Int. Ed. Engl.* **1982**, *21*, 711.
(18) Rösch, N. In *Electrons in Finite and Infinite Structures*; Phariseau, P., Scheire, L., Eds.; Plenum: New York, 1977; p 1.
(19) Case, D. A. *Annu. Rev. Phys. Chem.* **1982**, *33*, 151.
(20) Thornton, G.; Rösch, N.; Edelstein, N. M. *Inorg. Chem.* **1980**, *19*, 1304.
(21) Heera, V.; Seifert, G.; Ziesche, P. *J. Phys. B* **1984**, *17*, 519.
(22) Slater, J. C. *J. Chem. Phys.* **1964**, *41*, 3199.
(23) Rösch, N.; Klemperer, W. G.; Johnson, K. H. *Chem. Phys. Lett.* **1973**, *23*, 149.
(24) Norman, J. G., Jr. *Mol. Phys.* **1976**, *31*, 1191.
(25) Hohl, D. Diplom Thesis, Technische Universität München, 1985.
(26) Schwarz, K. *Phys. Rev.* **1972**, *85*, 2466; *Theor. Chim. Acta* **1974**, *34*, 225.

Table II. Xα–SW Ground-State Orbital Energies (in eV) and Orbital Charge Distributions[a] for $U(BH_4)_4$

		U									
orbital[b]	energy	s	p	d	f	total	B	H_b	H_t	inner sphere	outer sphere
$5t_2$	−6.07		0.026	0.397	0.027	0.450	0.155	0.031	0.014	0.339	0.011
2e	−6.86			0.603		0.603	0.121	0.037		0.234	0.005
$2t_1$	−8.28				0.833	0.833	0.062	0.020		0.083	0.002
$1t_2$	−8.98[c]		0.001	0.026	0.911	0.937	0.004	0.000	0.000	0.058	0.000
$3a_1$	−9.19[c]	0.028			0.834	0.861	0.011	0.002	0.001	0.123	0.002
$3t_2$	−11.71		0.043	0.016	0.010	0.068	0.298	0.058	0.112	0.437	0.027
$1t_1$	−11.88				0.159	0.159	0.236	0.170		0.432	0.003
$2a_1$	−12.18	0.073			0.023	0.095	0.305	0.012	0.141	0.416	0.030
1e	−12.53			0.195		0.195	0.196	0.144		0.463	0.003
$2t_2$	−12.69		0.008	0.153	0.003	0.165	0.208	0.126	0.026	0.467	0.009
$1t_2$	−16.96		0.031	0.071	0.007	0.109	0.333	0.118	0.017	0.419	0.004
$1a_1$	−17.45	0.099			0.017	0.116	0.302	0.120	0.012	0.416	0.003

[a] Fractions of orbital localization per type of muffin-tin region. For the metal sphere the contributions of the various partial waves are also shown. [b] The corelike orbitals U 6s and 6p, although included in the SCF process, are not included. [c] Highest occupied orbitals (with one electron each); all orbitals below are completely filled.

relativistic effects in the ligand field manifold of tetrahedral uranium complexes will be given elsewhere.[27]

Results and Discussion

We will start the discussion with a fairly detailed analysis of the molecular orbitals of uranium tetrakis(tetrahydroborate). Subsequently, we will compare the results for the series $M(BH_4)_4$ (M = Zr, Hf, Th, U) among each other and to the corresponding photoelectron spectra.

Molecular Orbitals of $U(BH_4)_4$. The relevant part of the molecular orbital spectrum of $U(BH_4)_4$ and the corresponding orbital charge distribution over the various muffin-tin regions are shown in Table II. In Figure 1 we compare the Xα–SW orbital energies of the complex with the corresponding level spectrum of an isostructural $(BH_4)_4$ cluster and of the molecule UCl_4. Also shown are spin–orbit averaged levels of the uranium atom from a relativistic Xα calculation.

The orbital spectrum of $U(BH_4)_4$ may be conveniently partitioned into four groups with energy and localization as criteria. At the high-energy end the first two levels, $5t_2$ and 2e, describe the empty U 6d orbitals. The next lower group, $2t_1$, $4t_2$, and $3a_1$, representing the highly localized U 5f orbitals, holds two electrons, in agreement with the expected $5f^2$ configuration of tetravalent uranium (see below). All lower levels are completely filled. The corresponding orbitals are mainly localized in the ligand region. They are most easily discussed in terms of BH_4^- valence orbitals. A clear description of how these molecular orbitals are constructed from ligand group orbitals has already been given[12,15] exploiting the isolability principle.[16,17] For convenience let us briefly summarize the main features.

The eight valence electrons of a tetrahedral BH_4^- moiety fill orbitals of a_1 and t_2 symmetry whose nodal properties are those of s and p orbitals of a monatomic ligand like Cl^-.[16] This analogy allows the immediate rationalization of the orbitals of a $(BH_4)_4$ cluster (see Figure 1). The s-like a_1 orbitals of the borohydride (mainly B 2s) give rise to cluster orbitals $1a_1$ and $1t_2$ at lower energies (ca. −16 eV), clearly separated from the remaining spectrum. The symmetry combinations of the p-like t_2 orbitals of BH_4^- generate the remaining cluster orbitals with bonding energies between about −10 and −11.5 eV. Conceptually, this p-type set may be further divided according to the bonding capabilities of the various group orbitals with respect to the metal atom present in the actual complex, in analogy to the distinction between p_σ and p_π orbitals of a monatomic ligand.[12] The orbitals $2a_1$ and $3t_2$ may be described as σ-type, and the orbitals $2t_2$, 1e, and $1t_1$ as π-type. Of course, for the two t_2 orbitals this is an idealization based on the contribution of the terminal hydrogen atoms measuring the σ character.[12] When the actual complex is formed, these $(BH_4)_4$ cluster orbitals undergo covalent mixing with the various metal orbitals. This leads to a characteristic

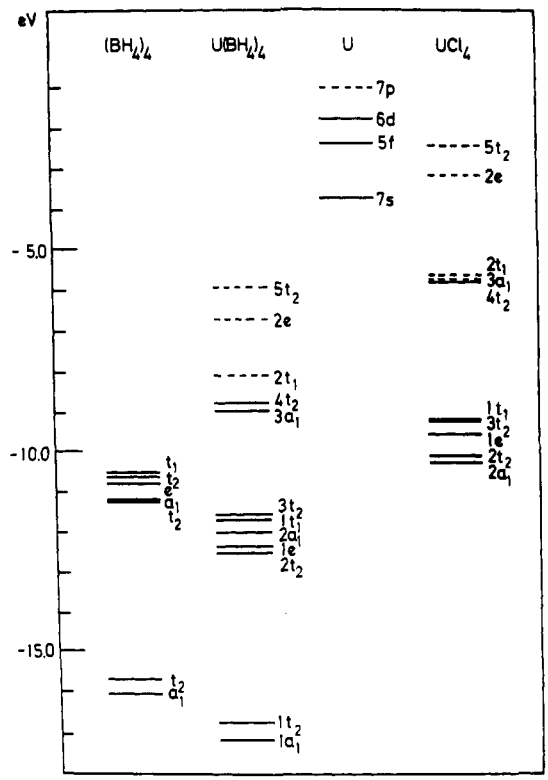

Figure 1. Xα–SW valence orbital energies for the tetrahedral complexes $U(BH_4)_4$ and UCl_4. Also shown for comparison are the orbital energies of the "empty" cluster $(BH_4)_4$ and of the U atom. Occupied orbitals are indicated by solid lines; empty ones, by dashed lines.

reordering within the p-like set, which will be discussed below in greater detail. However, the s-like and the p-like $(BH_4)_4$ levels may clearly be discriminated also in the spectrum of $U(BH_4)_4$, shifted downward by an average of about 1.4 eV (see Figure 1 and Table II).

The strongest metal–ligand interaction occurs in the π-type ligand orbitals $2t_2$, 1e, and $1t_1$, taking the orbital localization within the metal sphere as a gauge (see Table II). The metal–ligand bonding is dominated by the contribution of the U 6d orbitals to the $2t_2$ and the 1e orbitals. In Figure 2 we show contour maps of these two important orbitals in a plane containing two of the formal U–B–H_t bond axes and two of the bridging hydrogen atoms H_b. The π-bonding character of the 1e orbital is quite apparent. The $2t_2$ orbital must be regarded as a hybrid of the $t_2(\sigma)$ and the $t_2(\pi)$ $(BH_4)_4$ cluster orbitals discussed above. Through a distortion of the nodal surface away from the U–B bond axes a σ-type interaction between the metal and the boron atom becomes possible, strengthening the bonding character of this orbital. The σ contribution to this orbital may be read off from the delocal-

(27) Rösch, N.; Hohl, D.; Knappe, P.; Edelstein, N. M.; Ellis, D. E., to be submitted for publication.

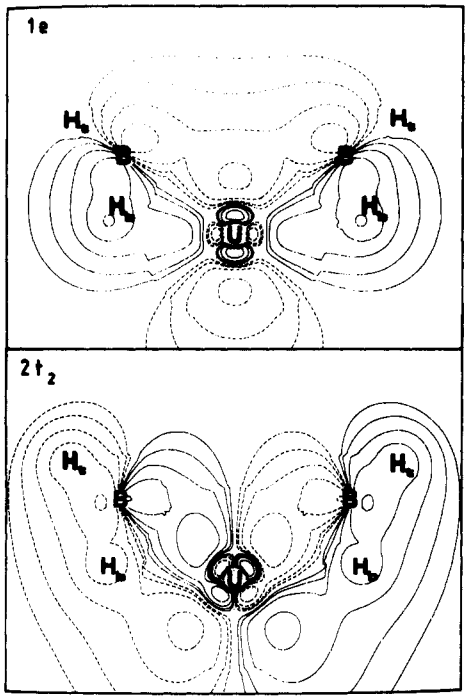

Figure 2. Contour plots for metal–ligand bonding orbitals of $U(BH_4)_4$, 1e and $2t_2$, in a plane containing the two bond axes U–B–H_t from the metal atom to the terminal hydrogen atoms H_t as well as two bridging hydrogen atoms H_b. Different signs of the orbitals are indicated by solid and dashed lines. The contour values used are (in au) 0.05, 0.1, 0.2, 0.4, and 0.8.

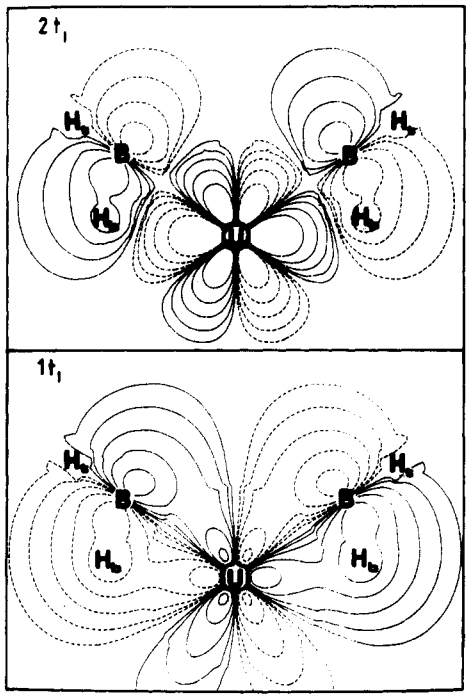

Figure 3. Contour plots for the metal–ligand bonding orbital $1t_1$ and its antibonding partner $2t_1$ of the ligand field manifold. The same layout has been used as in Figure 2.

ization onto the terminal hydrogen atoms. This σ contribution is also reflected in the level ordering, $2t_2$ below 1e, familiar for tetrahedral complexes.

The third orbital of the p_π-like set, the $1t_1$ orbital, would be nonbonding in a transition-metal complex. In $U(BH_4)_4$, however, it exhibits a substantial mixing with U 5f orbitals, as shown in Figure 3. If we accept the orbital localization in the metal sphere as a rough measure, we find less f covalency than in the corresponding orbitals of uranocene,[2] even when taking degeneracies into account (t_1 3 × 0.16 vs. e_{2u} 2 × 0.33). However, these

Table III. Ligand Field Parameters B_0^4 and B_0^6 and Corresponding One-Electron Energies for the 5f Orbitals of $M(BH_4)_4$ (M = U, Th; All Entries in cm^{-1})

	expt[a]	theory	
	$U(BH_4)_4$	$U(BH_4)_4$	$Th(BH_4)_4$
B_0^4	−2445	−1818	−634
B_0^6	−5371	−8051	−11718
$\epsilon(2t_1)^b$	+2402	+3488	+4955
$\epsilon(4t_2)^b$	−1697	−2207	−2842
$\epsilon(3a_1)^b$	−2116	−3842	−6326

[a] Model B.[13] [b] All orbital energies with respect to the corresponding center of gravity of the ligand field manifold.

numbers have to be interpreted with due caution since the radius of the uranium sphere is smaller by 0.09 Å in the present calculation. The two p-type orbitals involving the terminal hydrogens, $2a_1$ and $3t_2$, show much less ligand–metal interaction, the highest of the p-type manifold, $3t_2$, being almost nonbonding with respect to the metal.

Another way to measure the ligand–metal interaction is provided by the level shift as compared to the $(BH_4)_4$ cluster. Again we attribute the strongest interaction to the π-type ligand orbitals $2t_2$, 1e, and $1t_1$ (shifts: −1.44, −1.73, and −1.37 eV, respectively). The bonding shift of the other two p-like levels is significantly smaller ($1a_1$, −0.96 eV; $3t_2$, −1.10 eV). The present ordering of all p-type orbitals agrees quite well with that given previously[12] based on qualitative overlap arguments (π-bonding below σ-bonding levels). There is one slight difference, however. The $1t_1$ orbital falls between the two p_σ-like orbitals. This may be due to a strong antibonding ligand–ligand interaction not considered previously.[12] The ordering may also be affected by a differential muffin-tin effect.[25] In any case, the corresponding energy differences are rather small.

Finally, we would like to mention that the B 2s levels $1a_1$ and $1t_2$ also contribute to some extent to the metal–ligand bonding. Orbital contour maps, especially of the ligand-derived p-like levels (see Figure 2), reveal a strong direct interaction between the metal and the boron atoms that has already been conjectured for the analogous Np and Hf complexes on the basis of spectroscopically derived force constants.[6,12,31]

Let us now turn to the analysis of the ligand field levels $3a_1$, $4t_2$, and $2t_1$. Since a detailed discussion of the 5f manifold in tetrahedrally coordinated uranium complexes on the basis of Xα–SW calculations will be given elsewhere,[27] we summarize here those topics relevant to metal–ligand bonding. A U(IV) complex has the configuration $5f^2$. The interaction of these two electrons can certainly not be described adequately in a one-electron framework like the one underlying the present study because of the highly localized nature of the U 5f orbitals (see Table II). This may be confirmed by inspection of the ligand field Hamiltonian obtained from fitting the corresponding part of the optical spectrum of $U(BD_4)_4$.[13] Furthermore, the spin–orbit interaction, which has been neglected in the present treatment, should be larger than the ligand field splitting. The corresponding experimentally derived values are 0.77 and 0.56 eV, respectively.[13] Nevertheless, valuable insight may be gained from a judicious analysis of the present result for the ligand field levels.

The proper ground state of the present Xα-SW model is a $^3T_2$ state with the configuration $(3a_1\uparrow)^1(4t_2\uparrow)^1$ as obtained from a spin-polarized calculation. Accordingly, we have used the same orbital occupations for the evaluation of our non-spin-polarized calculation (see Table II). From the ligand field analysis[13] of $U(BD_4)_4$ a ^3E state is derived as the ground state with a $^3T_2$ state only 531 cm^{-1} higher, both showing a large $^3H_4$ contribution. The results of our model calculation are compatible with these experimental findings.

The splitting pattern of f orbitals in a tetrahedral ligand field considering only σ-type interactions is $t_1 < t_2 < a_1$.[28,29] In the

(28) Jørgensen, C. K.; Pappalardo, R.; Schmidtke, H. H. *J. Chem. Phys.* **1963**, *80*, 1422.

present calculation just the reverse ordering is found (see Table II). However, the calculated ordering reproduces correctly that derived from the one-electron part of the experimentally determined Hamiltonian[13] (see Table III).

Such a comparison is conveniently carried out by analyzing the calculated Xα–SW orbital energy differences in the 5f manifold in terms of the ligand field parameters B_0^4 and B_0^6 [30] (see Table III). No experimental data are available for $Th(BH_4)_4$. As in previous calculations[1,2] we find the overall splitting larger than the corresponding experimental value (for $U(BH_4)_4$ by a factor of about 1.6). The calculated (and experimental) level ordering may be rationalized as a combined effect of σ and π interaction with the ligands[29] on the one hand and a relativistic lowering of the $3a_1$ level (about 0.5 eV) due to its U 7s contribution on the other hand.[27] The $2t_1$ orbital has strong π-antibonding character (see Figure 3) and thereby reflects the f covalency of its bonding counterpart $1t_1$. Inspection of similar plots for the other ligand field orbitals $3a_1$ and $4t_2$ (not displayed) reveals their essentially nonbonding character (cf. Table II). This observation together with the fact that no direct relativistic shifts affect the $4t_2$ and $2t_1$ levels explains the calculated ordering $3a_1 < 4t_2 < 2t_1$.[27]

The U 5f spin–orbit constant ζ of the experimentally determined ligand field Hamiltonian furnishes a further test for the present calculation. From the optical analysis[13] a value of $\zeta = 1782$ cm^{-1} is derived, which leads to a reduction $k = 0.91$ from the U^{4+} free-ion value[32] of 1968 cm^{-1}. If we calculate the U 5f spin–orbit constant from the charge fraction localized within the uranium sphere[33] and average over the three ligand field levels, we obtain the value $\zeta = 1740$ cm^{-1}, in excellent agreement with the experimental result. The average f-like charge fraction within these orbitals of 0.87 is the quantity analogous to the orbital reduction factor. It should be mentioned that for fitting magnetic data of $U(BH_3CH_3)_4$ an improved agreement had been obtained by using an orbital reduction factor of 0.85.[13] The overall agreement of these features between experimental and calculated results is very satisfactory even when considering that the calculated charge fraction varies somewhat over the U 5f manifold and that this quantity depends on the sphere radii chosen.

Comment on the Isolobality of BH_4^- and Cl^-. The isolability[17] of borohydride and halide ligands has been used profitably to discuss the electronic structure of various compounds,[16] including the bonding in tetrakis(tetrahydroborate) complexes.[15] Here, we would like to highlight peculiarities of the BH_4^- ligand by pointing out more subtle differences with the Cl^- ligand. To this end we have included results of a quasi-relativistic Xα–SW calculation of UCl_4[27] in Figure 1. The level ordering in the Cl 2p manifold differs significantly from that of the p-like ligand-derived levels in $U(BH_4)_4$. Whereas the latter may be taken to indicate nearly equal importance of σ and π bonding, one finds for UCl_4 the classical ordering of a tetrahedral complex with dominant σ bonding, $2a_1$ and $2t_2$ being below the π-bonding levels 1e, $1t_1$, and $3t_2$. In the borohydride complex the pure π-bonding levels lie about 0.9 eV below the essentially nonbonding level $3t_2$; the corresponding value for the chloride complex is only 0.4 eV, pointing toward a weaker π interaction.

To enhance the preceding we present in Figure 4 contour maps for the orbitals $2t_2$ and 1e of UCl_4, which may be compared to the corresponding orbitals of $U(BH_4)_4$ in Figure 2. The difference of the two $2t_2$ orbitals is quite striking. For UCl_4 it is purely σ bonding, confirming the discussion given above. The 1e orbital of $U(BH_4)_4$ exhibits a stronger π bond, just as inferred from the orbital energy differences. Comparing Figures 2 and 4, one may trace the strong π-bonding capability of the borohydride ligand

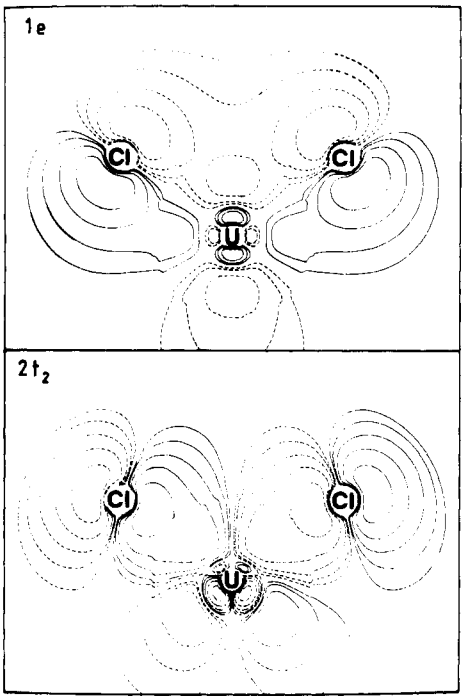

Figure 4. Contour plots for the two metal–ligand bonding orbitals of UCl_4. The orbitals shown correspond to those of Figure 2, 1e and $2t_2$. The same layout has been used as in Figure 2.

to a favorable distortion of the p-like orbitals mediated via the bridging hydrogen atoms. This effect is clearly lacking for a monatomic halide ligand. A similar distortion of the chlorine p orbital could only be induced through a sizable d-orbital participation, as shown in **1**.

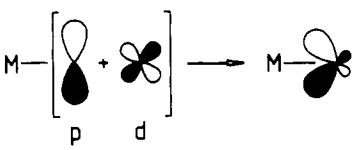

1

Partial waves of d character in the Cl sphere had been included in the UCl_4 calculation,[27] but there is no discernible polarization. Somewhat pointedly, we may call the distortion of the π-bonding p-type orbitals in the borohydride moiety "structurally induced d polarization".

Comparison of Different Metal Tetrahydroborates. Two of the various metal tetrakis(tetrahydroborates) that have been included are transition-metal compounds (M = Zr, Hf), and two are actinide compounds (M = Th, U). One expects the results in each group to be rather similar,[4] the main differences between the groups being caused by f-orbital participation and relativistic effects in the actinide compounds.[34] These expectations are born out to a considerable extent as one discovers from the Xα–SW ground-state-orbital spectra. In Figure 5 we compare that part of the spectrum containing the ligand-derived B 2s and p-like levels on one hand and the metal-derived valence d and f (for M = Th, U only) on the other. These metal valence levels contain no electrons for M = Zr, Hf, and Th.

Aside from the two 5f electrons in the ligand field manifold of the uranium complex, there are two major differences between the transition-metal and the actinide compounds, both concerning the p-like ligand-derived levels. Their energies are spread out significantly more for M = Zr and Hf than for M = Th and U (1.9 vs. 1.0 eV, respectively), and the highest level is $1t_1$ for M = Zr and Hf and $3t_2$ for M = Th and U. Thus, there is a change in the character of the HOMO when going from Hf to Th. Both

(29) Warren, K. D. *Inorg. Chem.* **1977**, *16*, 2008.
(30) Wybourne B. G. *Spectroscopic Properties of Rare Earths*; Wiley: New York, 1965.
(31) Keiderling, T. A.; Wozniak, W. T.; Gay, R. S.; Jurkowitz, D.; Bernstein, E. R.; Lippard, S. J.; Spiro, T. G. *Inorg. Chem.* **1975**, *14*, 576.
(32) van Deurzen, C. H. H.; Rajnak, K.; Conway, J. G. *J. Opt. Soc. Am. B: Opt. Phys.* **1984**, *1*, 45.
(33) Boring, M.; Wood, J. H. *J. Chem. Phys.* **1979**, *71*, 32. Goursot, A.; Chermette, H. *Chem. Phys.* **1982**, *69*, 329.
(34) Pyykkö, P.; Desclaux, J. P. *Acc. Chem. Res.* **1979**, *12*, 276.

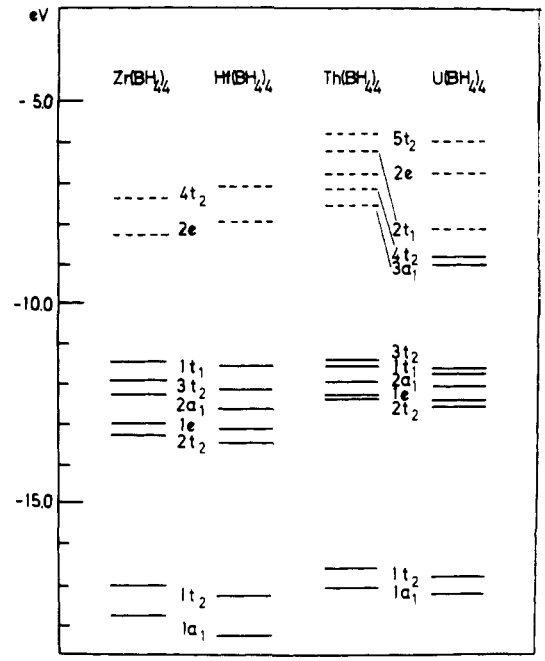

Figure 5. Xα–SW valence orbital energies for various metal tetrakis(tetrahydroborates). Occupied orbitals are indicated by solid lines; empty ones, by dashed lines.

Table IV. Comparison of d- and f-Type Charge Fractions Localized in the Metal Sphere for the Ligand-Derived p-like Orbitals of the Complexes $M(BH_4)_4$

MO	partial wave	metal			
		Zr	Hf	Th	U
$1t_1$	d				
	f	0.020	0.019	0.098	0.159
$3t_2$	d	0.043	0.048	0.014	0.016
	f	0.001	0.001	0.005	0.010
$2a_1$	d				
	f	0.002	0.001	0.015	0.023
1e	d	0.278	0.248	0.197	0.195
	f				
$2t_2$	d	0.199	0.176	0.156	0.153
	f	0.000	0.000	0.003	0.003
av[a]	d	0.107	0.118	0.075	0.075
	f	0.005	0.005	0.028	0.045
	f/d	0.05	0.04	0.37	0.60

[a] Weighted average according to the degeneracy of the various orbitals; contribution to the total metal occupation is 24 times this value.

observations may be connected with qualitative and quantitative differences of the metal valence levels and their involvement in covalent ligand–metal bonding. To support this argument we have collected in Table IV the d- and f-type charge fractions localized in the metal sphere of the various $M(BH_4)_4$ complexes for the ligand-derived p-like orbitals.

The order among the two highest lying orbitals, $3t_2$ and $1t_1$, is obviously correlated with the corresponding metal population. In each case the highest lying level is almost nonbonding. For the two transition metals a small d contribution lowers the $3t_2$ orbital, for the two actinides a sizable f contribution clearly favors the bonding in the $1t_1$ orbital (see Table IV). The d-type charge fraction in the $2t_2$ and 1e orbitals is definitely lower for the two actinide complexes and, concomitantly, the covalent energy lowering smaller. This effect accounts for the significantly smaller width of the p-type manifold in these compounds.

The difference in the metal-derived part of the orbital spectrum of the two f-element compounds is reminiscent of that found between thorocene and uranocene.[1,2] The gap between the highest ligand-derived and the lowest 5f-type levels is in both types of compounds larger for Th than for U, the values in the borohydride complexes being about twice those of the sandwich compounds.

Table V. Partial-Wave Analysis for Valence Electrons of the Metal Atom in $M(BH_4)_4$

	Zr	Hf	Th	U	
				f^{0a}	f^{2b}
s	0.360	0.446	0.333	0.344	0.372
p	0.479	0.526	0.499	0.497	0.498
d	3.057	2.786	2.249	2.219	2.245
f	0.155	0.168	0.735	1.155	2.899
total	4.051	3.926	3.816	4.215	6.014

[a] Only those ligand-derived orbitals are included that correspond to the ones occupied in the other three complexes ($1a_1$–$3t_2$). [b] Standard orbital occupation including $(3a_1)^1(4t_2)^1$.

The same trend is observed for the ligand field splitting of the metal 5f orbitals: 0.91 and 0.99 eV for $U(BH_4)_4$ and uranocene, respectively; 1.42 and 1.52 eV for the corresponding Th complexes. The strength of the ligand field is somewhat overestimated in the present model.[1] For $Th(BH_4)_4$ the metal 6d-derived 2e level falls energetically within the 5f manifold.

A comparison of the overall metal–ligand bonding in the various metal tetrahydroborates can best be accomplished on the basis of a partial-wave analysis of the metal sphere population in the valence levels (see Table V). Since the complexes $M(BH_4)_4$ (M = Zr, Hf, Th) exhibit formally the valence configuration d^0 (d^0f^0 for Th), this metal population arises from the ligand-derived levels and may therefore be taken as a measure for the covalent interaction in these complexes. For M = U, two configurations are shown in Table V, the true configuration d^0f^2 and, for ease of comparison, d^0f^0 where the two electrons in the ligand field levels have not beeen included. When analyzing the data in Table V, one has to keep in mind that these occupations depend on the metal sphere radius chosen (see Table I) which, unlike the previous study of the di-π-[8]annulene compounds,[1-3] is not uniform. Quantitative conclusions from Table V should therefore be drawn only with a certain reservation. Qualitative trends are expected to be invariant with respect to reasonable variations of the metal sphere radii.

The metal s and p orbital contribution to covalent bonding is small and fairly constant for all compounds, with a small but noticeable deviation of s population in Hf (see the discussion below). Not unexpectedly, we find the covalent ligand–metal bonding dominantly effected by the metal d orbitals with a slightly but definitely larger d occupation in transition-metal complexes. To appreciate this one should keep in mind that the corresponding muffin-tin sphere radii are smaller. Whereas the f occupation is very small for M = Zr and Hf, one finds a sizable f contribution for M = Th and U (see also the f/d relation in Table IV). The f covalency of the uranium complex is by far the largest in the series. When the U $5f^2$ electrons are excluded, the f occupation reaches a value of 1.16, which is about half the d occupation (see Table V).

A comparison with the corresponding results for thorocene and uranocene is quite instructive.[1,2] There, f covalency was also significantly larger for the uranium than for the thorium compound. Comparing the covalent ligand bonding in sandwich and in corresponding borohydride complexes, we note larger f and smaller d occupations in the metal spheres of the organometallic compounds, the differences being roughly 0.6 and −0.6, respectively, for both metals. This comparison is somewhat hampered by the different metal sphere size used in the previous study[1] (r(Th) = r(U) = 1.788 Å). Nevertheless, one may state that f covalency is certainly not a unique characteristic of di-π-[8]-annulene f-element compounds although they seem to exhibit it to an unusually large degree. Otherwise, we may describe the bonding in the actinide tetrakis(tetrahydroborates) as fairly similar to that in the classical tetrahedral transition-metal complexes, as far as the metal is concerned. However, this neglects the strong π-bonding effects to typical for the borohydride ligand,[27] as discussed above.

To conclude this comparison let us comment on the total metal population in the borohydride complexes (see Table V). If we

Table VI. Comparison of Calculated Transition-State Orbital Energies and Experimental Ionization Potentials for the Series $M(BH_4)_4$ (M = Zr, Hf, Th, U; All Energies in eV) and DVM–Xα Results for M = Zr

$Zr(BH_4)_4$			$Hf(BH_4)_4$		$Th(BH_4)_4$		$U(BH_4)_4$	
DVM-Xα[a]	TSOE[b]	expt[c]	TSOE[b]	expt[c]	TSOE[d]	expt[e]	TSOE[d]	expt[f]
					(5f)		11.73	9.58
9.7	13.85 ($1t_1$)	11.6	13.97	11.7	13.58 ($3t_2$)	12.0	13.77	11.9
10.8	14.25 ($3t_2$)	12.7	14.51	12.6	13.79 ($1t_1$)		14.01	
11.1	14.62 ($2a_1$)		15.00		14.05 ($2a_1$)		14.25	
11.7 ($2t_2$)	15.45 (1e)	13.4	15.59	13.6	14.53 (1e)	13.0	14.66	13.0
13.2 (1e)	15.67 ($2t_2$)	13.8	15.91	13.9	14.62 ($2t_2$)		14.79	
16.0	19.51 ($1t_2$)	18.3	19.80	18.4	18.93 ($1t_2$)	17.5	19.09	17.78, 18.29
17.0	20.25 ($1a_1$)	19.4	20.82	19.8	19.33 ($1a_1$)	18.5	19.57	19.04
	(4f)		27.59	26.11				

[a] Transition-state orbital energies of ref 15. Level designation is given only where the level ordering differs from that in the present work. [b] This work. Level designation valid both for M = Zr and for M = Hf; 4f level for M = Hf only. [c] Reference 15. [d] This work. Level designations valid both for M = Th and for M = U; 5f level for M = U only. [e] Reference 35. [f] Reference 12.

were to derive a metal charge from this quantity (Zr, −0.05; Hf, 0.08; Th, 0.18; U, −0.01), we would deduce increasing ionicity of these complexes in the order Zr < Hf and U < Th. The values of these atomic charges seem to make their interpretation questionable. The two comparisons offered are for metals of similar size and may therefore be accepted as meaningful. For the two actinides a very similar charge differences has been found previously.[2]

Comparison with Photoelectron Spectra. Experimental photoionization potentials for the $M(BH_4)_4$ complexes (M = Zr,[12,15] Hf,[12,15] Th,[35] U[12]) are compared in Table VI with calculated transition-state orbital energies (TSOE) of the present investigation. Agreement between calculated and measured ionization potentials is only moderately satisfactory, the absolute values of the TSOEs being uniformly too large by about 2 eV. Relative spacings (width of the p-like manifold, gap between p-like levels and B 2s energies, splitting of the two B 2s levels, gap between the 5f and first ligand-derived band in $U(BH_4)_4$) are reproduced rather well in all four cases.

The systematic deviation of the calculated results are undoubtedly errors due to the muffin-tin approximation to the electronic potential underlying the SW formalism.[18] From geometrical inspection it is quite obvious that tetrahedral complexes exhibit quite an "open" structure. This comes to bear here in a twofold way, both for the ligands and for the composite system. Better agreement with experiment could have been obtained by allowing overlapping muffin-tin spheres.[18,23,25]

Also included in Table VI are TSOEs of a previous LCAO–DVM–Xα calculation on $Zr(BH_4)_4$.[15] Although the DVM–Xα is free of muffin-tin errors, the results for the Zr complex also deviate systematically from experiment. The DVM–Xα ionization energies are almost uniformly too small by about 2 eV. Part of this discrepancy might be caused by the choice of the STO basis functions in this DVM calculation. Furthermore, taking the energy difference between the maxima of the highest and the lowest shoulder as a measure for the width of the first band in the PE spectrum (2.2 eV), we find this quantity grossly overestimated in the DVM calculation (3.5 eV). The Xα–SW result (1.8 eV), on the other hand, slightly underestimates the experimental value, which is a well-known deficiency of this method.[18]

Both the DVM–Xα and the Xα–SW TSOEs lead to the same assignment[15] of the PE spectrum of $Zr(BH_4)_4$ with a single exception: the ordering of the p-like 1e and $2t_2$ levels is reversed (see Table VI). It is quite conceivable that the SW ordering is wrong, the splitting of the two levels being only 0.2 eV. However, a differential muffin-tin error on this splitting of almost 2 eV, as implied by the DVM results, would represent an extreme case according to our experience. Indeed, recent DVM–Xα calculations[36] using numerical basis functions (similar to those employed by the SW formalism) confirm almost quantitatively the present SW result for $Zr(BH_4)_4$, both for the width of the ligand p manifold and for the ordering of the p-like 1e and $2t_2$ levels. A further discussion of these calculations will be given elsewhere.[36]

Before further discussion of the shape and any detailed assignment of the first broad band in the PE spectrum (the second band for M = U), it seems fitting to mention results of ab initio Greens function investigation on strong many-body and vibronic coupling effects in PE spectra.[37] It has been pointed out that such effects can completely prevent a molecular orbital interpretation especially of broad bands because the spectral strength of a one-electron transition may be spread over a significant part of the spectrum. Even peak structures of a broad band can be misleading.[37]

With this in mind we want the information in Table VI on the first PE band to be read as a statement on propensities rather than a definite assignment of certain subpeaks within this broad band.[15] This is to mean that we expect ionization processes related to the orbitals $1t_1$, $3t_2$, and $2a_1$ to contribute preferentially to the low-energy side of the band and those related to the 1e and $2t_2$ orbitals more to the high-energy side. We are then able to offer an explanation for the narrower width of this band in the actinide complexes as compared to the transition-metal complexes. In a comparative analysis of the corresponding orbitals we had found that the metal d constribution to ligand–metal bonding is reduced in the actinide complexes and that their 5f orbitals do participate in this bonding (see the previous section and Table V). Both effects work toward a narrower PE band. The first lowers the ionization energy calculated for the d bonding levels 1e and $2t_2$; the second raises the ionization energy of the otherwise nonbonding $1t_1$ level. One has to remember, however, that spin–orbit effects due to metal populations increase the width of this band in the actinide complexes. By perturbation theory one estimates an additional broadening of about 0.5 eV from the metal contributions.

The first assignment given for the PE spectra of these complexes was based on qualitative molecular orbital arguments.[12] It agrees quite well with the interpretation given here with the exception of the $1t_1$ agreement. In the present study we group this orbital energetically together with the levels $2a_1$ and $3t_2$.

The conspicuous similarity between the spectra of the zirconium and the hafnium complexes is to be expected from their chemical properties.[4] The present calculation reflects this fact, but it also reproduces their subtle differences. The experimental ionization potentials of the hafnium compound are generally higher by 0.1 eV; the corresponding shifts in the TSOEs average to about 0.25 eV. Experimentally, there is one exception to the similarity of the two spectra. The peak at 19.4 eV in $Zr(BH_4)_4$ is shifted to 19.8 eV in $Hf(BH_4)_4$. The exceptional size of this shift is also reproduced in the present calculation for the $1a_1$ TSOE (0.67 eV). Two explanations have been suggested previously: (a) a reduced shielding of the supposedly corelike B 2s level in $Hf(BH_4)_4$ and thus a somewhat lower electron density on B[15] and (b) a larger amount of direct metal–boron interaction in the hafnium compound.[12]

(35) Green, J. C.; Shinomoto, R.; Edelstein, N. *Inorg. Chem.*, following paper in this issue.
(36) Hohl, D.; Ellis, D. E.; Rösch, N., submitted for publication.
(37) Köppel, H.; Cederbaum, L. S.; Domcke, W.; Shaik, S. S. *Angew. Chem., Int. Ed. Engl.* **1983**, *22*, 210.

Our calculation supports alternative b. The difference between the Zr and the Hf complexes is a relativistic effect. The Hf 6s orbital lies lower than the Zr 5s orbital due to the relativistically increased effective mass of the electron.[34] Consequently, the Hf 6s orbital will mix stronger into the occupied a_1 orbitals of the borohydride complex. This is most noticeable for the $1a_1$ orbital where the metal population increases from 0.11 for M = Zr to 0.15 for M = Hf and leads to an enlarged covalent energy lowering. The effect in the $2a_1$ orbitals is smaller, but the corresponding shift of 0.38 eV is still larger than average. The total s population of Hf and Zr also reflect this difference (see Table V).

Acknowledgment. The authors are grateful to Dr. N. Edelstein for stimulating discussions and for his encouraging interest. This work has been supported in part by the Deutsche Forschungsgemeinschaft and by the Leonhard-Lorenz-Stiftung.

Registry No. $Zr(BH_4)_4$, 12370-59-1; $Hf(BH_4)_4$, 37274-93-4; $Th(BH_4)_4$, 12523-76-1; $U(BH_4)_4$, 102630-71-7.

Contribution from the Inorganic Chemistry Laboratory, Oxford OX1 3QR, England, and Materials and Molecular Research Division, Lawrence Berkeley Laboratory, University of California, Berkeley, California 94720

Photoelectron Spectra of Metal Tetrakis(methyltrihydroborates) and Thorium Tetrakis(tetrahydroborate)

Jennifer C. Green,*† Ron Shinomoto,‡ and Norman Edelstein*‡

Received December 9, 1985

He I and He II photoelectron spectra of $M(BH_3CH_3)_4$ (M = Zr, Hf, Th, U) and that of $Th(BH_4)_4$ in the vapor phase have been obtained. Assignments of the bands based on the Xα-SW calculations of Hohl and Rösch for $M(BH_4)_4$ are given.

Introduction

The volatile metal tetrahydroborates ($M(BH_4)_4$; M = Zr, Hf, Th, Pa, U, Np, Pu) have been the subject of structural, vibrational, optical, photoelectron (PE), and theoretical studies.[1-8] For the actinide tetrahydroborates, one of the major questions has been the extent of the f orbitals' involvement in the bonding in these complexes.[5,6] Unfortunately, the first three members of the actinide borohydride series, $Th(BH_4)_4$, $Pa(BH_4)_4$, and $U(BH_4)_4$, are polymeric in the solid state with a metal site symmetry much lower than the T_d symmetry found in the vapor phase.[9] Recently, the volatile compounds $M(BH_3CH_3)_4$ where M = Zr, Th, U, and Np have been synthesized and structurally characterized.[10] These studies have shown the metal ion is at a site of approximately T_d symmetry in the solid state. Magnetic measurements for both $U(BH_3CH_3)_4$ and $Np(BH_3CH_3)_4$ have been interpreted on this basis.[11-13]

Photoelectron spectra of $Zr(BH_4)_4$, $Hf(BH_4)_4$, and $U(BH_4)_4$ have been published and discussed previously by two groups.[5,6] Quasi-relativistic Xα-SW calculations of $M(BH_4)_4$ (M = Zr, Hf, Th, U) have been described and reproduced the ionization energies satisfactorily except for a uniform shift.[8] We report in this paper the photoelectron spectra of $M(BH_3CH_3)_4$ (M = Zr, Hf, Th, U) and, for completeness, $Th(BH_4)_4$. These spectra are assigned on the basis of their similarities to the $M(BH_4)_4$ compounds and the results of the Xα-SW calculations.

Experimental Section

Photoelectron spectra were obtained on a PES Laboratories 0078 spectrometer, with data collection either on an XY recorder or by means of a RML 380Z microprocessor. The spectra were calibrated by reference to Xe, N_2, and He. The methyltrihydroborate samples were prepared as described previously.[10] $Th(BH_4)_4$ was prepared as described by Katz and Hoekstra.[14]

Results

He I and He II spectra were obtained for $Th(BH_4)_4$ and $M(BH_3CH_3)_4$ (M = Zr, Hf, Th, U) in the vapor phase. Ionization energy (IE) data are given in Table I and representative spectra shown in Figures 1-5. The individual points give the raw data, whereas the solid line is a least-squares fit to these points.[15] As most of the bands were broad and featureless, they are not well characterized by the chosen IE, and identification of trends necessitates comparison of the whole band shape and position.

The PE spectra of the thorium and uranium tetrakis(methyltrihydroborates) show two bands (A and B) in the region 10-16 eV. $U(BH_3CH_3)_4$ has an additional band (f) at 8.3 eV, which shows a substantial intensity increase in the He II spectrum, and may be associated with ionization of the $5f^2$ electrons. Three further high-IE bands (C, D, E) are clearly defined in the He II spectrum of $Th(BH_3CH_3)_4$ (see Figure 3).

In contrast, the Zr and Hf analogues have an additional low-energy band (A') with a maximum at circa 10.7 eV. Intensity comparisons suggest that this ionization comprises part of the first band A in the spectra of the actinide tetrakis(methyltrihydroborates). Otherwise, the spectra are very similar to those of their heavier congeners. There is a very low intensity band (f) at 24.7 eV visible in the He II spectrum of $Hf(BH_3CH_3)_4$. A similar band was found at 26.1 eV for $Hf(BH_4)_4$[5] and assigned to ionization of the 4f shell. The kinetic energy of band f, 16.1 eV, is very close to that of the He self-ionization band, 16.2 eV. In all the spectra measured here the latter tended to be suppressed at the pressure used for data collection and could only be observed at low com-

* To whom correspondence should be addressed.
† Inorganic Chemistry Laboratory.
‡ University of California.

(1) For a review of work prior to 1977 see: Marks, T. J.; Kolb, J. R. *Chem. Rev.* **1977**, *77*, 263.
(2) Bernstein, E. R.; Keiderling, T. A. *J. Chem. Phys.* **1973**, *59*, 2105.
(3) Banks, R. H.; Edelstein, N. M.; Spencer, B.; Templeton, D. H.; Zalkin, A. *J. Am. Chem. Soc.* **1980**, *102*, 620.
(4) Banks, R. H.; Edelstein, N. M. *J. Chem. Phys.* **1980**, *73*, 3589.
(5) Downs, A. J.; Egdell, R. G.; Orchard, A. F.; Thomas, P. D. P. *J. Chem. Soc., Dalton Trans.* **1978**, 1755.
(6) Hitchcock, A. P.; Hao, N.; Werstiuk, N. H.; McGlinchey, M. J.; Ziegler, T. *Inorg. Chem.* **1982**, *21*, 793.
(7) Mancini, M.; Bougeard, P.; Burns, R. C.; Mlekuz, M.; Sayer, B. G.; Thompson, J. I. A.; McGlinchey, M. J. *Inorg. Chem.* **1984**, *23*, 1072.
(8) Hohl, D.; Rösch, N. *Inorg. Chem.*, preceding paper in this issue.
(9) Bernstein, E. R.; Hamilton, W. C.; Keiderling, T. A.; LaPlaca, S. J.; Lippard, S. J.; Mayerle, J. J. *Inorg. Chem.* **1972**, *11*, 3009.
(10) Shinomoto, R.; Gamp, E.; Edelstein, N. M.; Templeton, D. H.; Zalkin, A. *Inorg. Chem.* **1983**, *22*, 2351.
(11) Rajnak, K.; Gamp, E.; Shinomoto, R.; Edelstein, N. M. *J. Chem. Phys.* **1984**, *80*, 5942.
(12) Rajnak, K.; Banks, R. H.; Gamp, E.; Edelstein, N. *J. Chem. Phys.* **1984**, *80*, 5951.
(13) Gamp, E.; Edelstein, N. *J. Chem. Phys.* **1984**, *80*, 5963.
(14) Hoekstra, H. R.; Katz, J. J. *J. Am. Chem. Soc.* **1949**, *71*, 2488.
(15) The smoothing method used fits a weighted polynomial to a number of points successively across the data set. The polynomial is weighted so that the fit is equivalent to a least-squares fit over each group of points. See: Savitzky, A.; Golay, M. J. E. *Anal. Chem.* **1964**, *36*, 1627.

0020-1669/86/1325-2718$01.50/0